Supporting Information

for

Synthesis and Bonding Analysis of Pentagonal Bipyramidal Rhenium Carboxamide Oxo Complexes

Noah D. McMillion,[1] Quinton J. Bruch,[1] Chun-Hsing Chen,[1] Faraj Hasanayn[2,], and Alexander J. M. Miller[1,*]*

[1] Department of Chemistry, University of North Carolina at Chapel Hill, Chapel Hill, North Carolina 27599-3290, United States

[2] Department of Chemistry, American University of Beirut, Beirut 1107 2020, Lebanon

* Corresponding author information: F.H. (fh19@aub.edu.lb); A.J.M.M. (ajmm@email.unc.edu)

Table of Contents

I. NMR Spectra

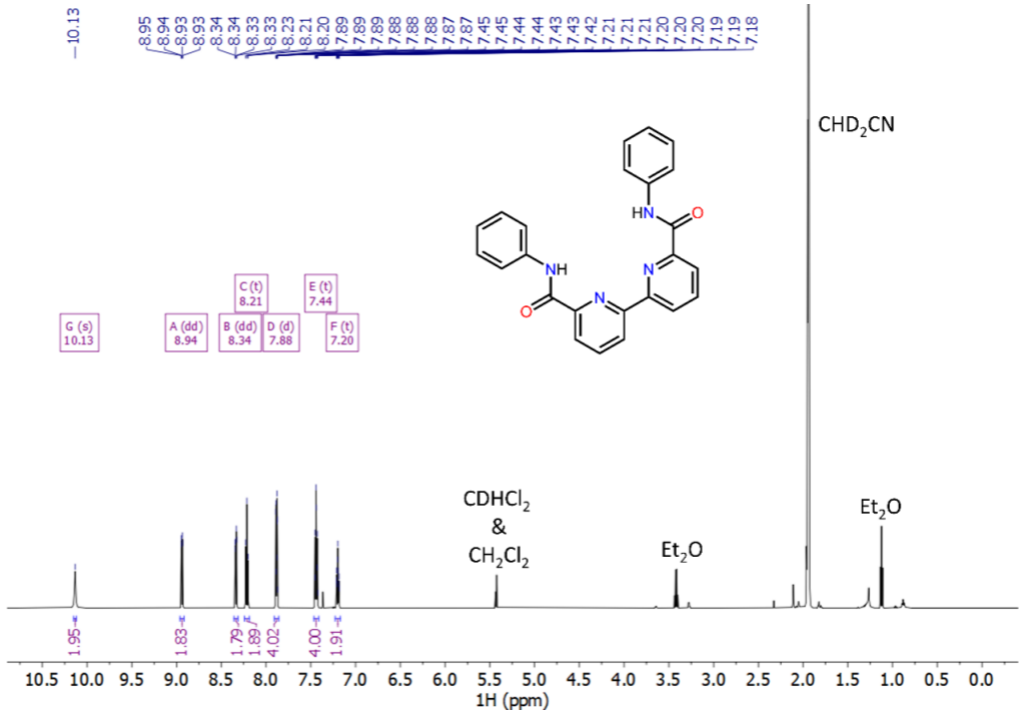

Figure S1. ^{1}H NMR spectrum (600 MHz) of H_2^{Ph}bpy-da in CD_3CN and 8% CD_2Cl_2 by volume.

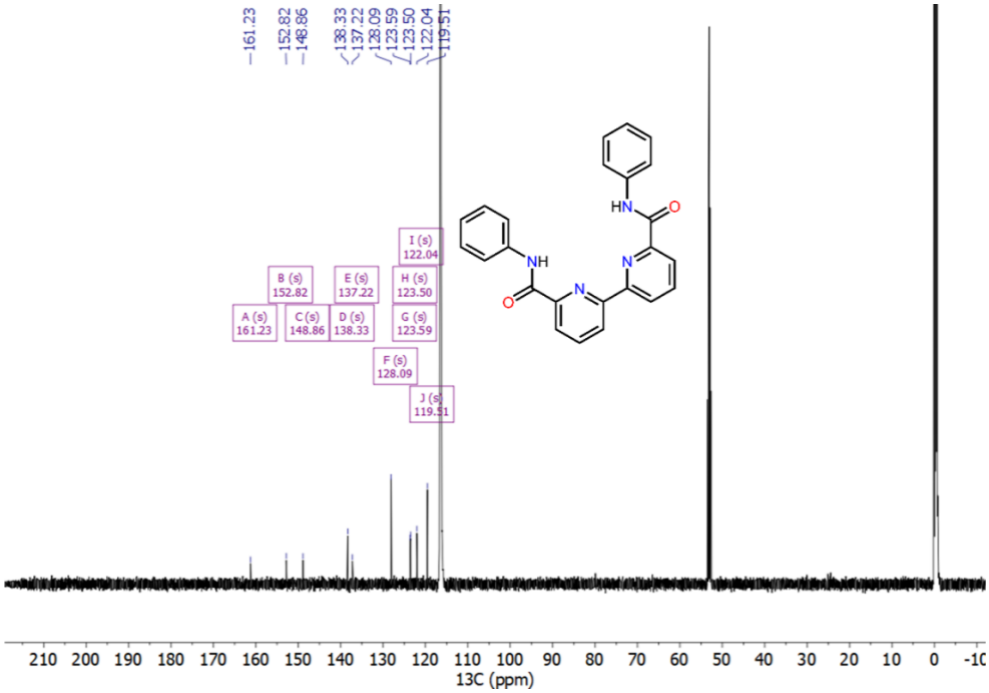

Figure S2. $^{13}C\{^{1}H\}$ NMR spectrum (151 MHz) of H_2^{Ph}bpy-da in CD_3CN and 8% CD_2Cl_2.

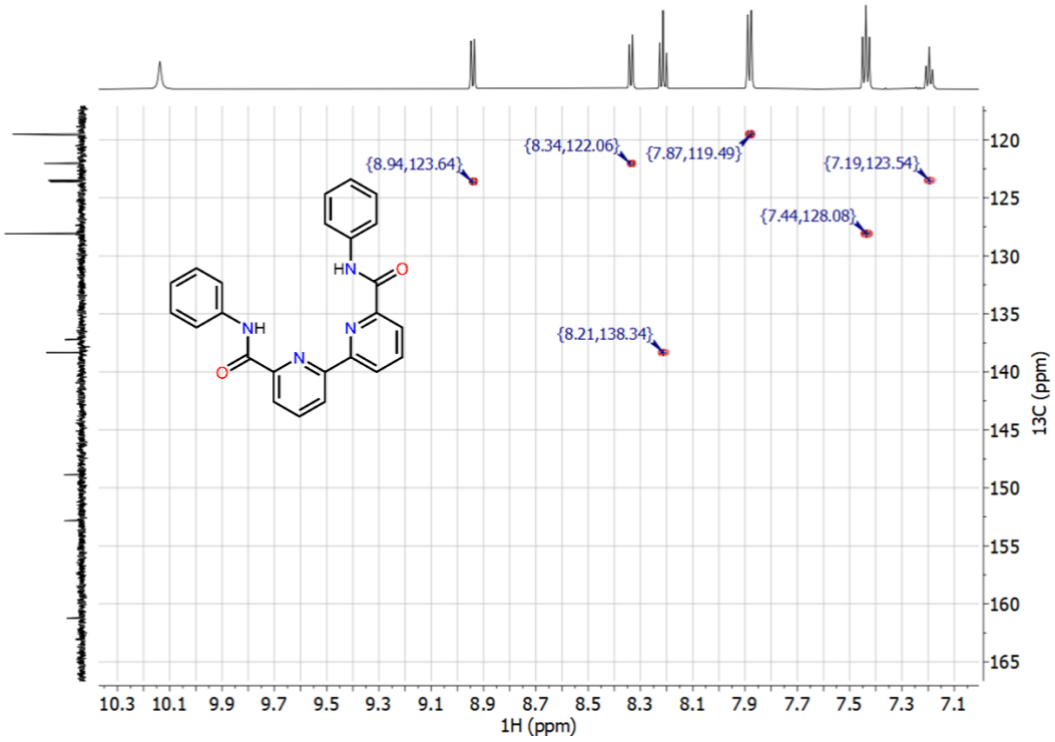

Figure S3. ^{1}H-^{13}C HSQC NMR spectrum (aromatic region) of H_2^{Ph}bpy-da in CD_3CN and 8% CD_2Cl_2.

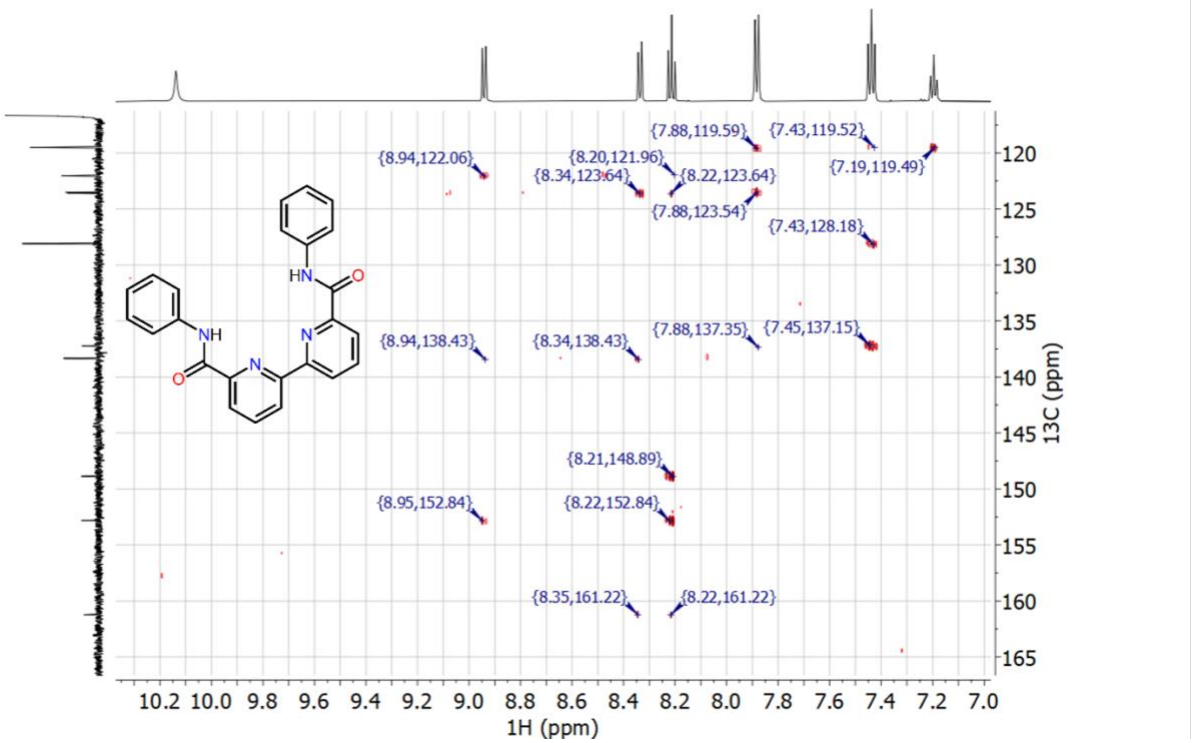

Figure S4. ^{1}H-^{13}C HMBC NMR spectrum (aromatic region) of H_2^{Ph}bpy-da in CD3CN and 8% CD_2Cl_2.

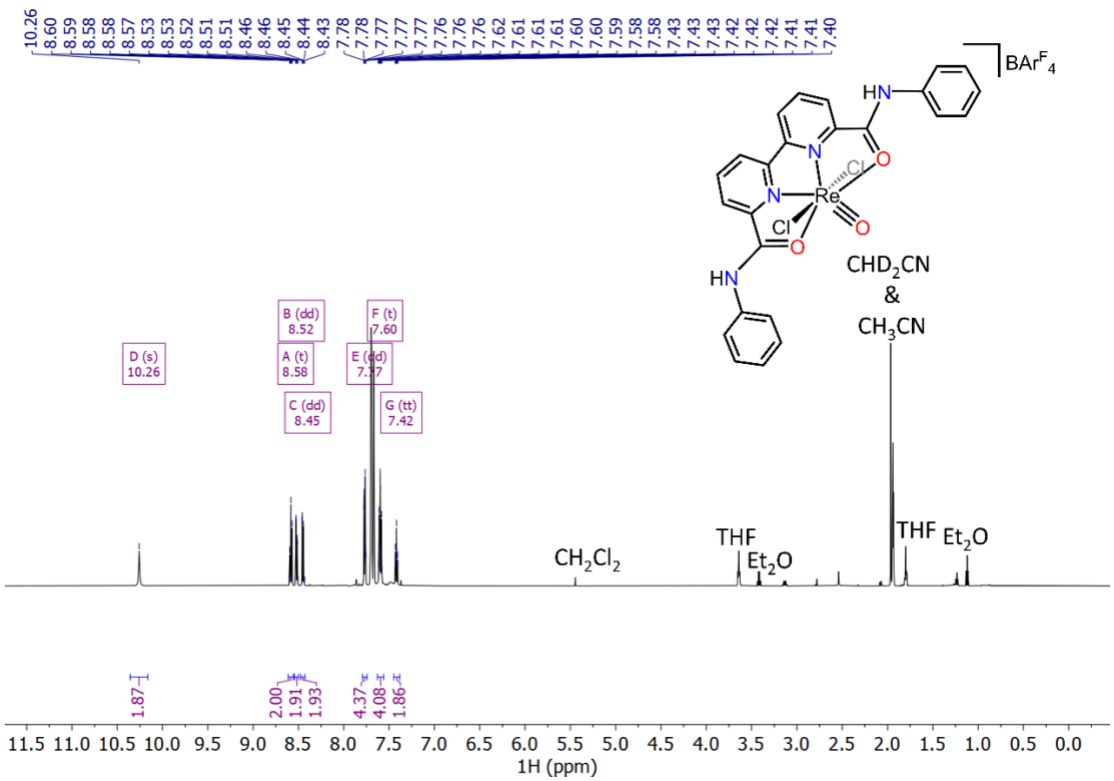

Figure S5. ^{1}H NMR spectrum (600 MHz) of [**1**][BAr$^F_4$] in CD$_3$CN.

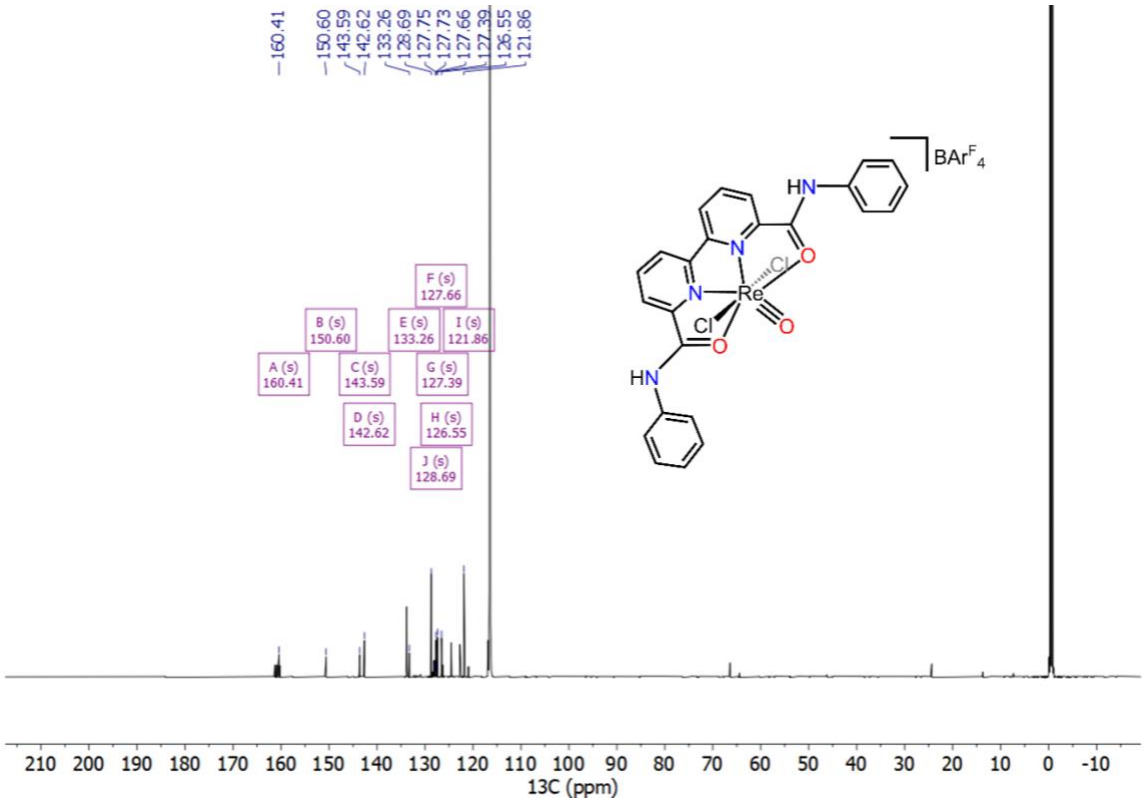

Figure S6. ^{13}C{^{1}H} NMR spectrum (151 MHz) of [**1**][BAr$^F_4$] in CD$_3$CN.

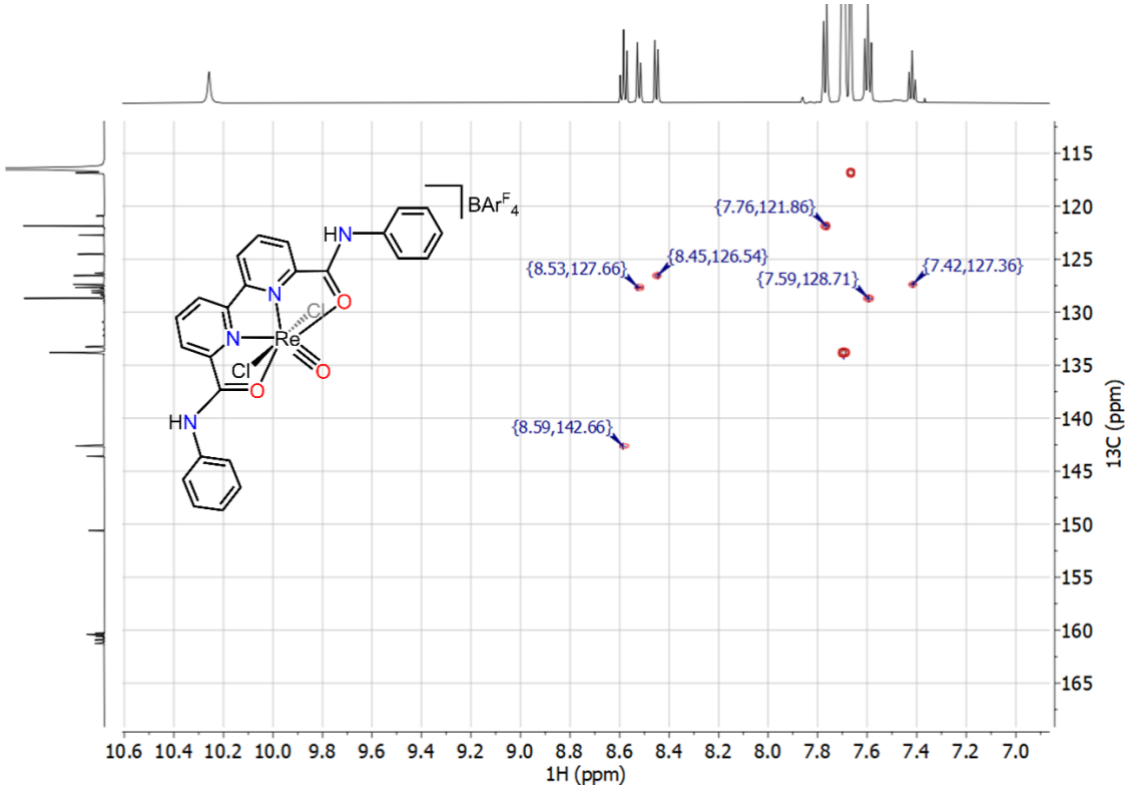

Figure S7. ^{1}H-^{13}C HSQC NMR spectrum (aromatic region) of [**1**][BAr$^F_4$] in CD_3CN.

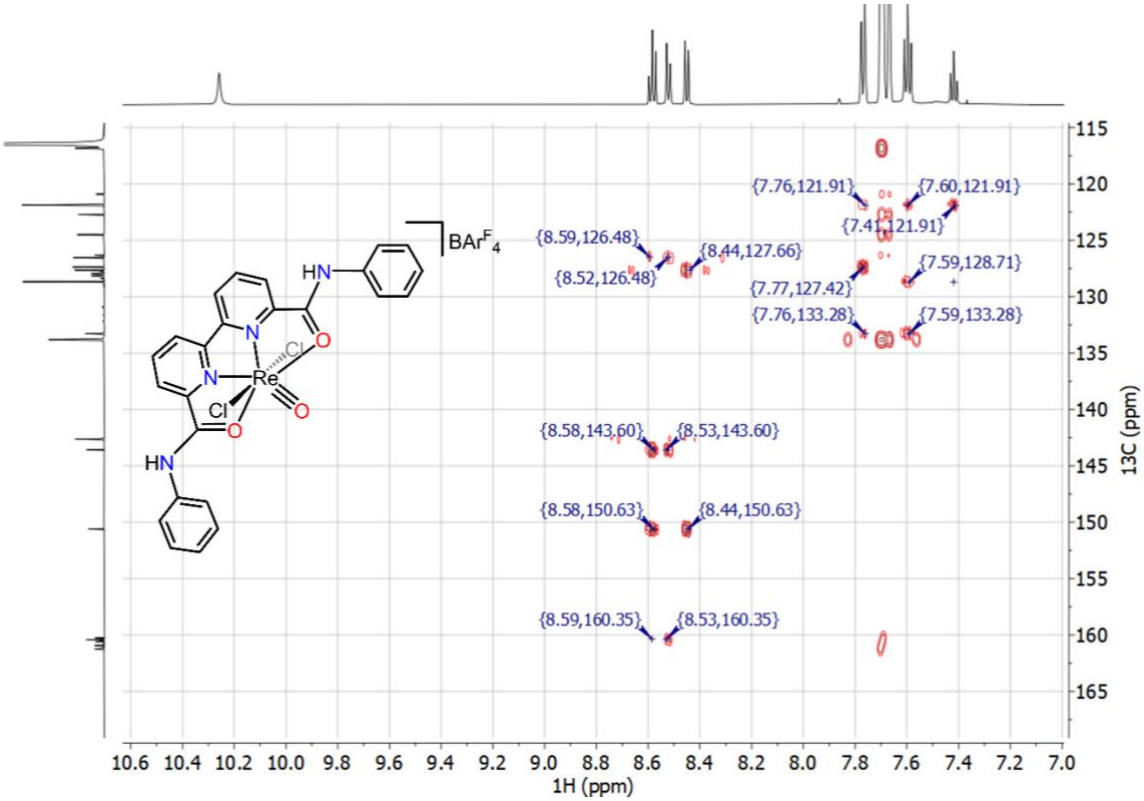

Figure S8. ^{1}H-^{13}C HMBC NMR spectrum (aromatic region) of [**1**][BAr$^F_4$] in CD_3CN.

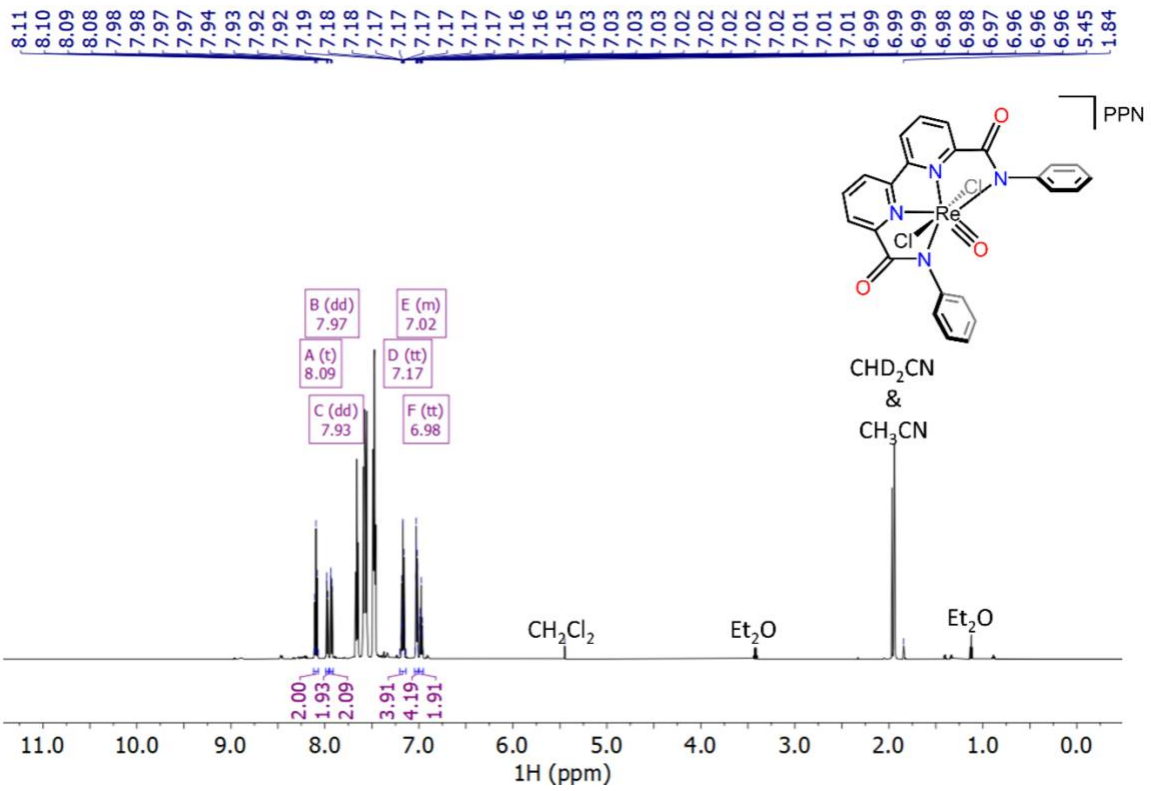

Figure S9. ^{1}H NMR spectrum (600 MHz) of [PPN][**2**] in CD_3CN.

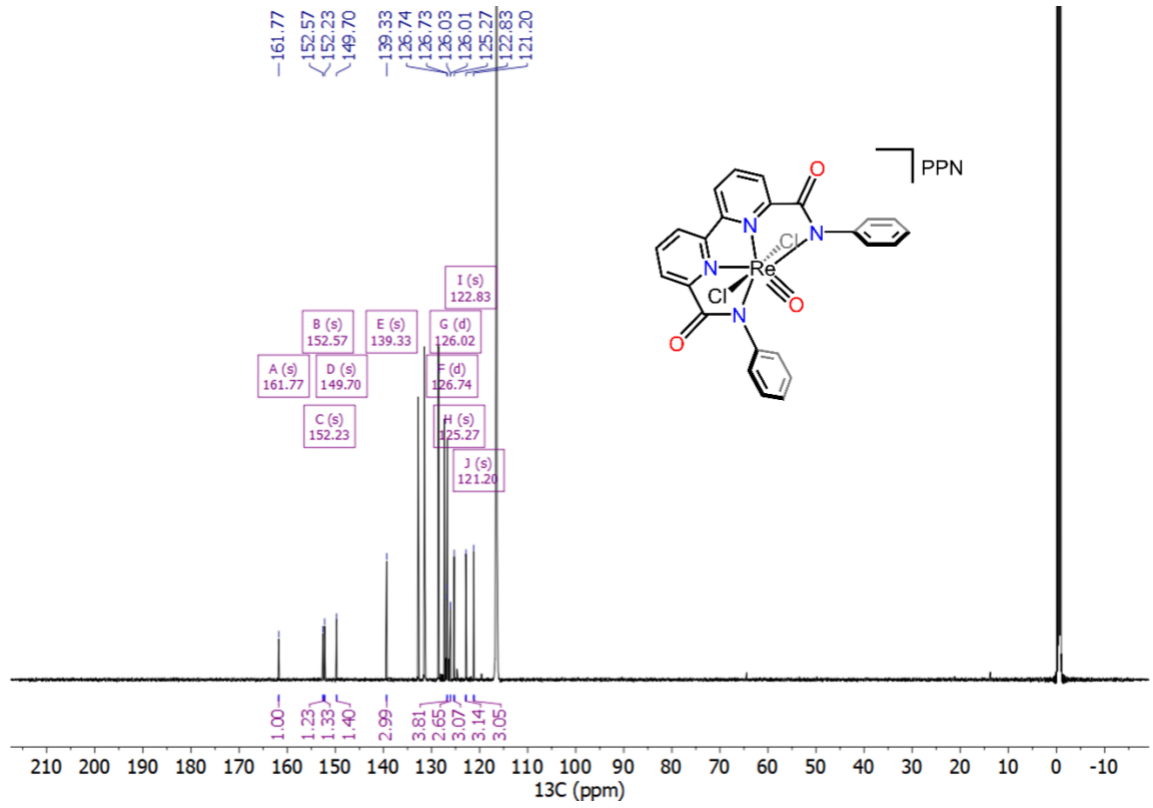

Figure S10. $^{13}C\{^{1}H\}$ NMR spectrum (151 MHz) of [PPN][**2**] in CD_3CN.

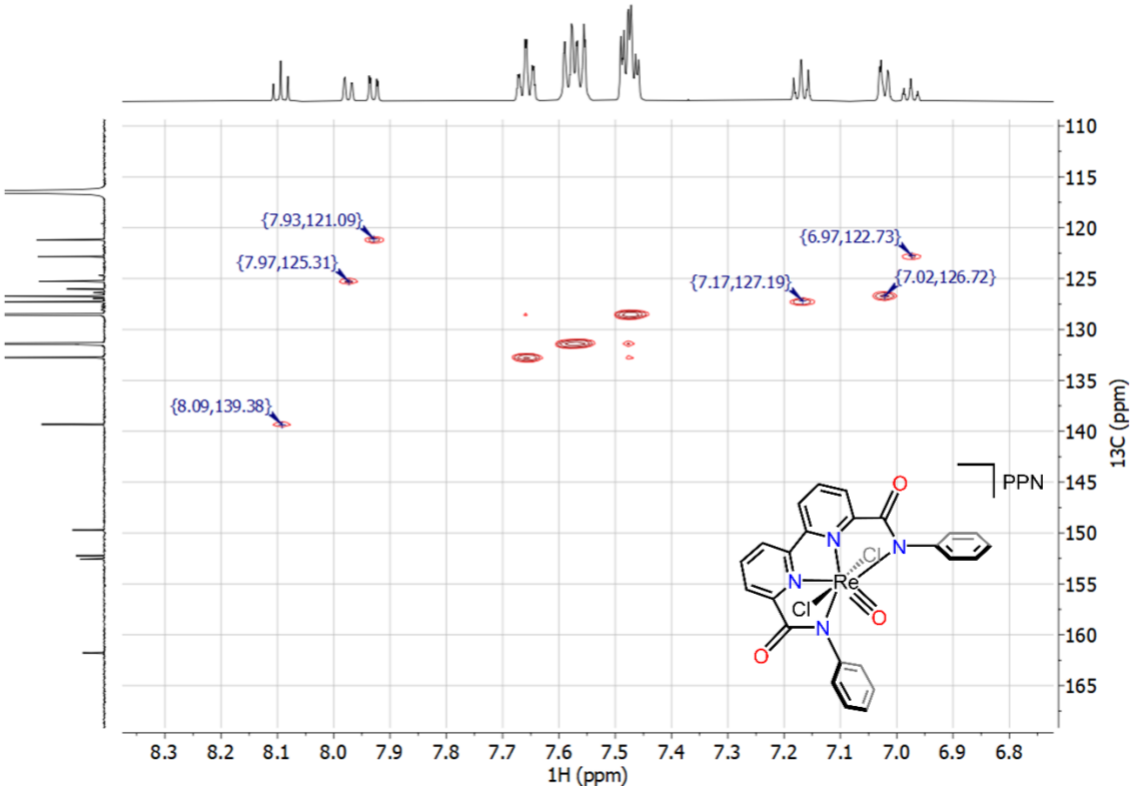

Figure S11. ^{1}H-^{13}C HSQC NMR spectrum (aromatic region) of [PPN][**2**] in CD_3CN.

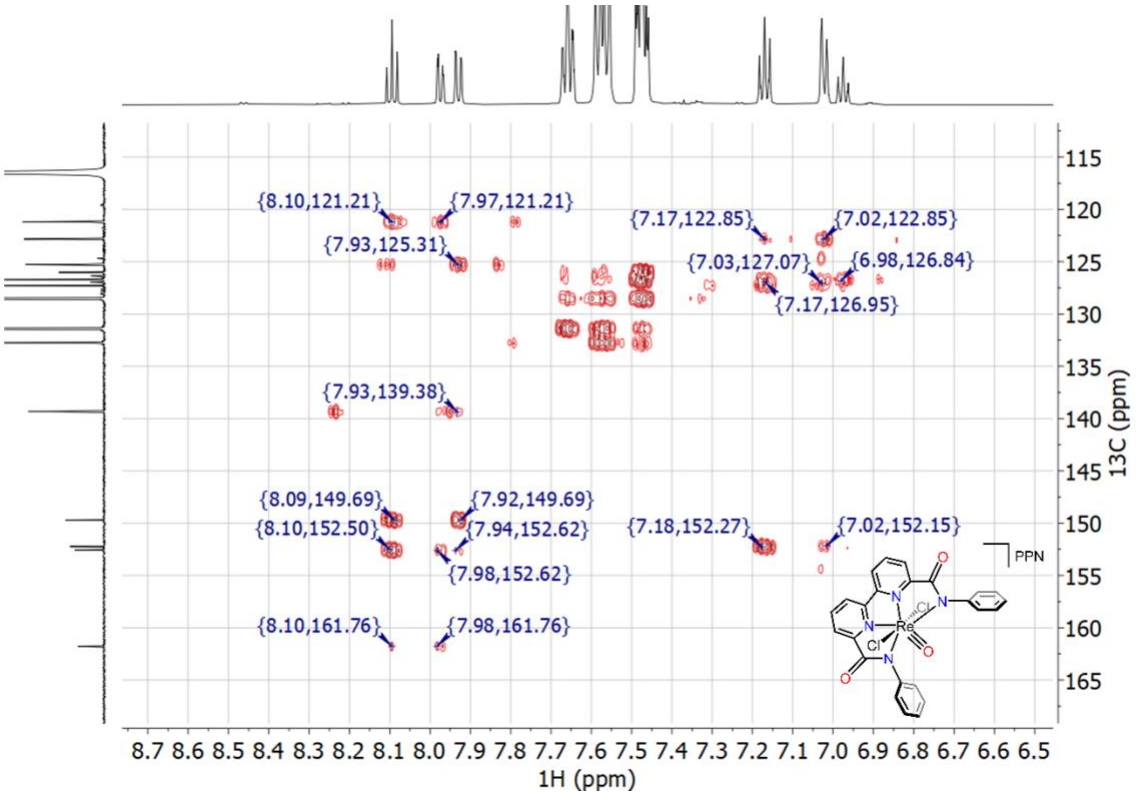

Figure S12. ^{1}H-^{13}C HMBC NMR spectrum (aromatic region) of [PPN][**2**] in CD_3CN.

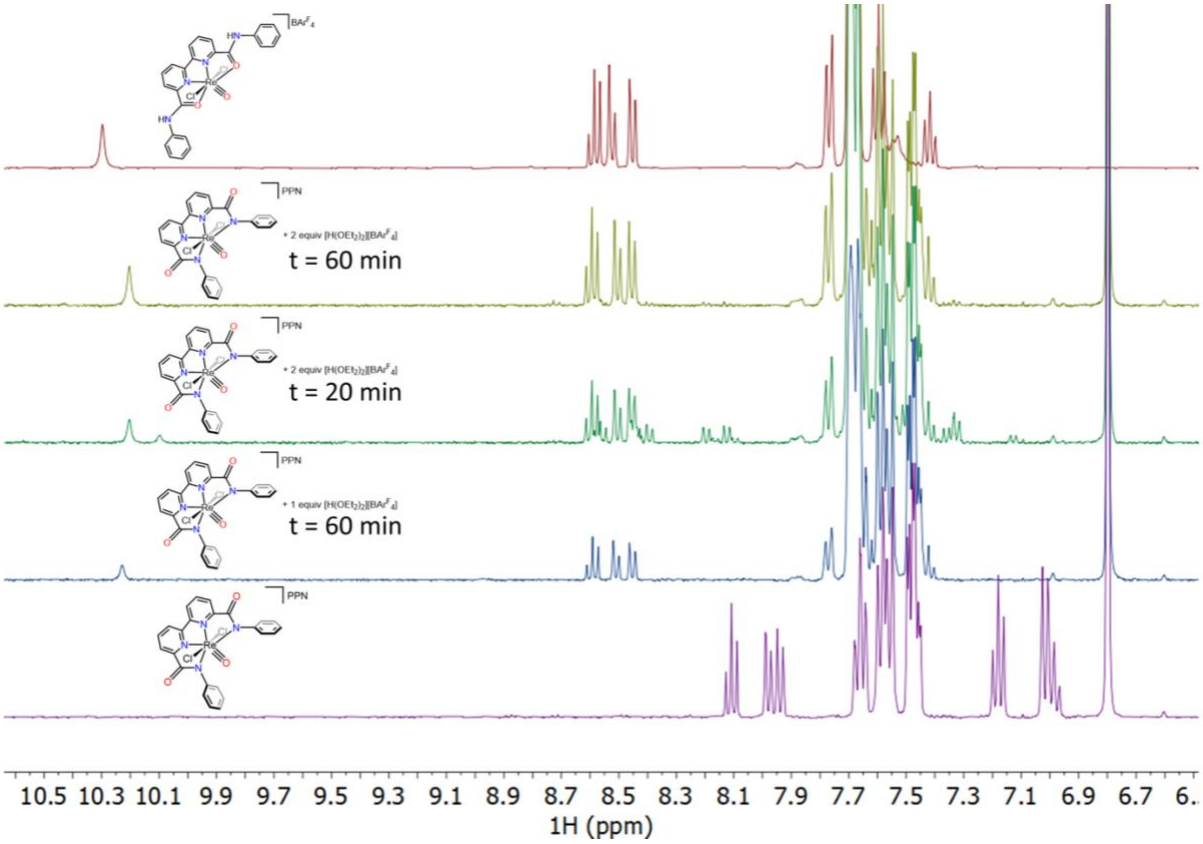

Figure S13. NMR spectroscopic analysis of the protonation of [PPN][**2**]. Purple (bottom): ^{1}H NMR spectrum (400 MHz) of [PPN][**2**]. Blue: ^{1}H NMR spectrum (400 MHz) of [PPN][**2**] and 1 equiv $[H(OEt_2)_2][BAr^F{}_4]$ after reacting for 1 hour. Dark green: ^{1}H NMR spectrum (400 MHz) of [PPN][**2**] and 2 equivalents of $[H(OEt_2)_2][BAr^F{}_4]$ after reacting for 20 min. Light green: ^{1}H NMR spectrum (400 MHz) of [PPN][**2**] and 2 equivalents of $[H(OEt_2)_2][BAr^F{}_4]$ after reacting for 1 hour. Red (top): ^{1}H NMR spectrum (600 MHz) of [**1**]$[BAr^F{}_4]$. Mesitylene (18 mM) was added as an internal standard.

II. Infrared Spectra

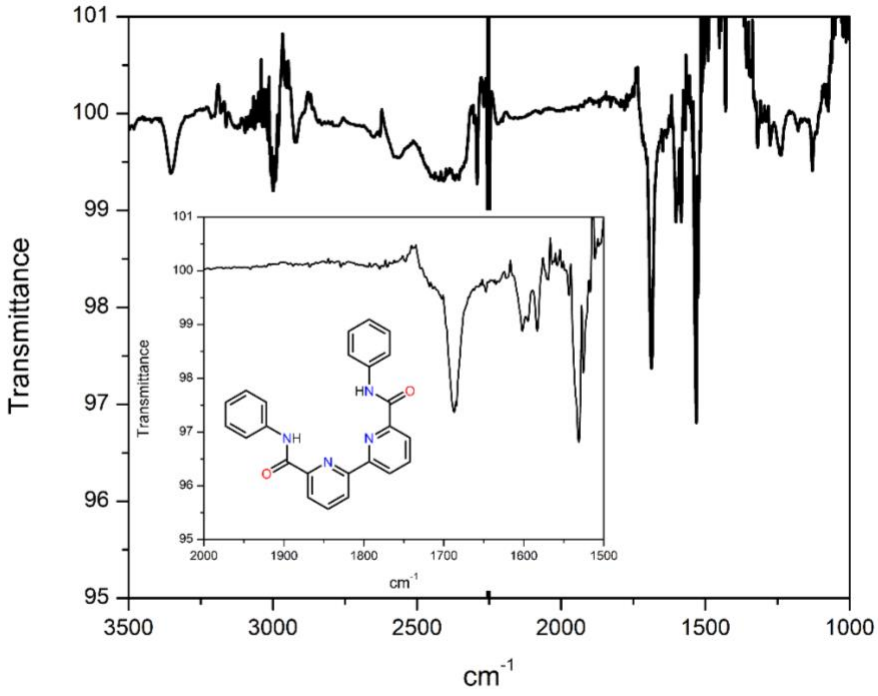

Figure S14. Solution-phase FTIR spectrum of H_2^{Ph}bpy-da in MeCN and 8% CH_2Cl_2. Inset: Carbonylic region.

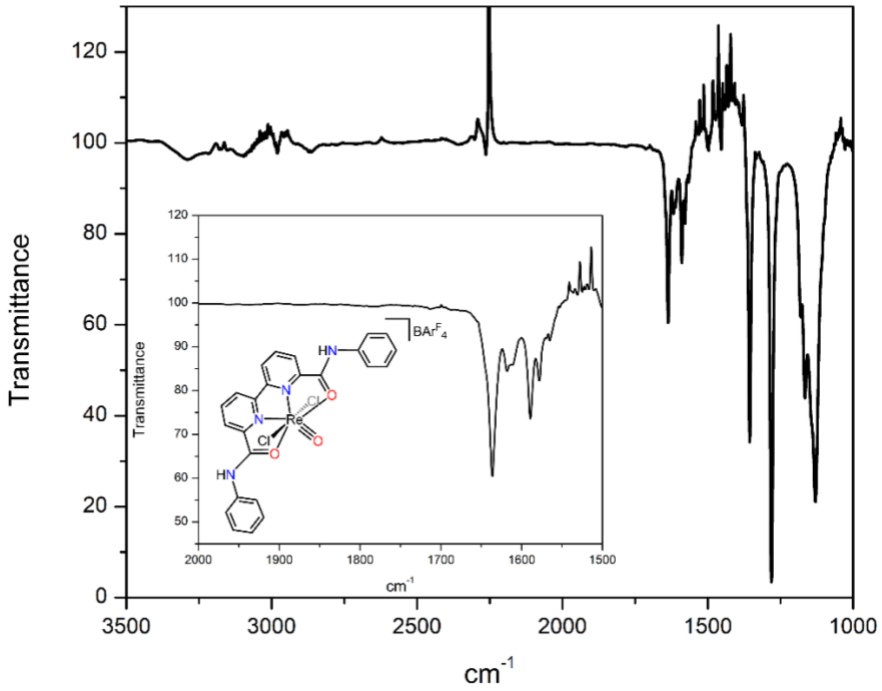

Figure S15. Solution-phase FTIR spectrum of [**1**][BAr^F_4] in MeCN. Inset: Carbonylic region.

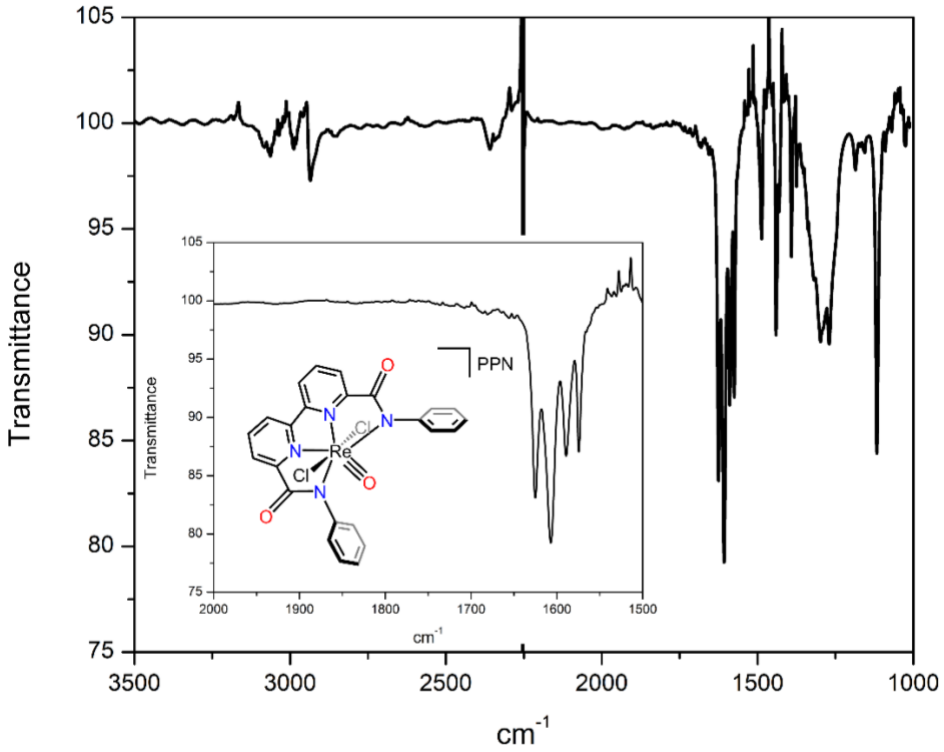

Figure S16. Solution-phase FTIR spectrum of [PPN][**2**] in MeCN. Inset: Carbonylic region.

III. Crystallographic Details

H_2^{Ph}bpy-da – 22021

Crystallographic Details. The crystal sample was grown at room temperature in air via slow vapor diffusion of diethyl ether into a saturated acetonitrile solution. From this sample, a colorless crystal of approximate dimensions 0.05 mm x 0.1 mm x 0.1 mm was placed onto the tip of a MiTeGen loop before mounting the crystal in a Bruker D8 VENTURE diffractometer. Subsequent X-ray study was performed under an N_2 cryo-stream at 150 K.

Data Collection. Preliminary cell constants were first determined using reflections harvested from a set of 180 frames. These sets of frames were positioned such that a half sphere coverage in the reciprocal space was surveyed to allow determination of initial orientation matrices from 1408 reflections. Next, data collection was performed using a Mo Kα radiation source (graphite monochromator) with frame time of 2.5 seconds and a detector distance of 4.9 cm. A randomly oriented region of reciprocal space was surveyed to achieve complete data with a redundancy of 6.3. Sections of frames were collected in 0.5º steps as ω and φ scans. During reduction, data to a resolution of 0.81 Å were considered. Cell constants after data reduction were calculated from the xyz centroids of 8252 strong reflections after integration (SAINT).[1] Absorption correction was applied to the intensity data (SADABS).[2] For additional crystal and refinement information, refer to Table S1.

Structure Solution and Refinement. A space group of *P2₁/c* was determined based on intensity statistics and systematic absences. Superflip[3] was used to solve the structure which was then refined (full-matrix least-squares) using the Oxford University Crystals software package for Windows.[4] Non-hydrogen atoms were refined with anisotropic displacement parameters before placing hydrogen atoms in ideal geometric positions. Additional refinement cycles then performed

in which these hydrogen atoms were refined as riding atoms with individual relative isotropic displacement parameters. The final full-matrix least-squares refinement converged with R1 = 0.0674 and wR2 = 0.1233 (F^2, all data).

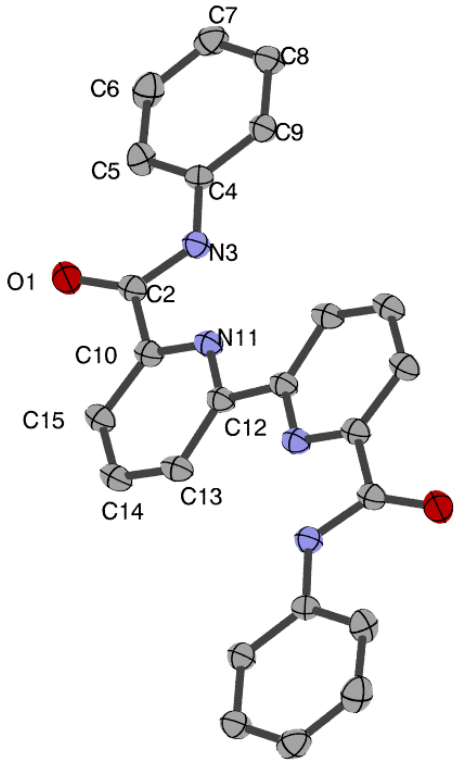

Figure S17. Crystal structure of H_2^{Ph}bpy-da with atom labels on the asymmetric unit.

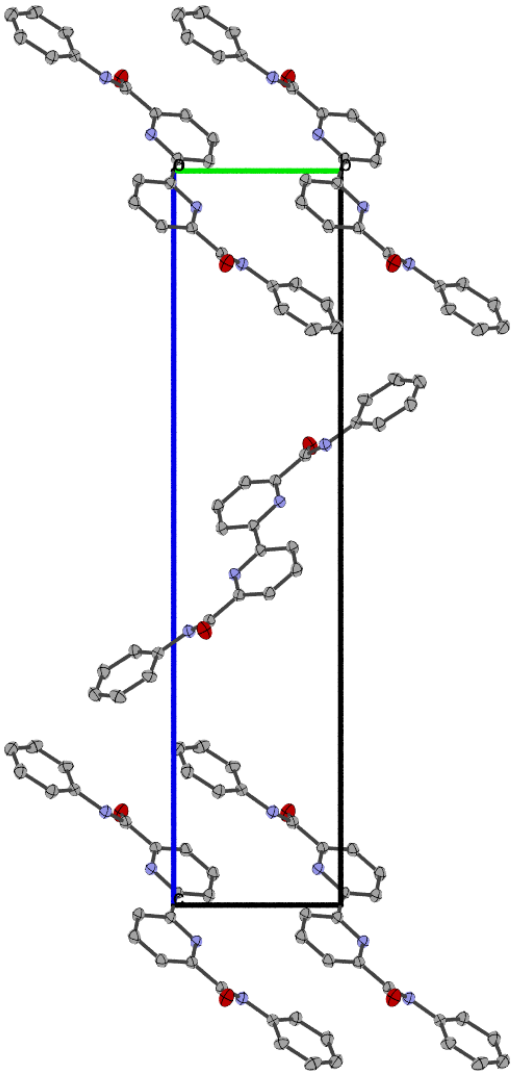

Figure S18. Cell plot of H_2^{Ph}bpy-da, viewed along the a axis.

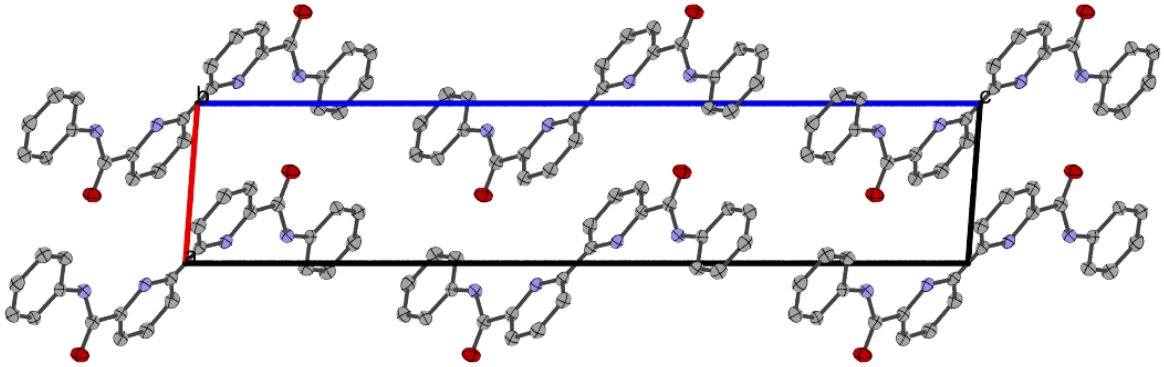

Figure S19. Cell plot of H_2^{Ph}bpy-da, viewed along the b axis.

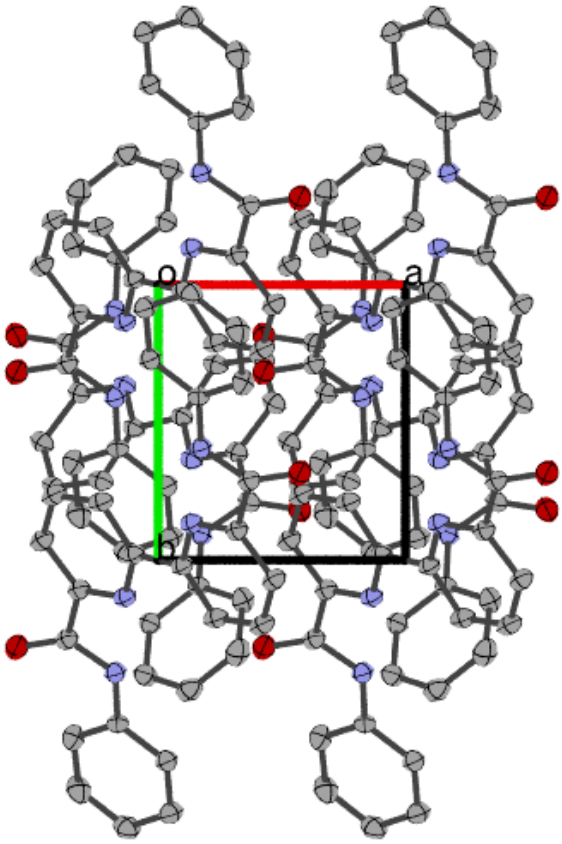

Figure S20. Cell plot of H_2^{Ph}bpy-da, viewed along the c axis.

Table S1. Crystal data and structure refinement for 22021.

Identification code	22021
Empirical formula	$C_{24}H_{18}N_4O_2$
Formula weight / g/mol	394.43
Temperature/K	150
Crystal system	Monoclinic
Space group	*P2₁/c*
a/Å	5.5694(3)
b/Å	6.1838(3)
c/Å	27.2625(10)
α/°	90
β/°	94.3510(15)
γ/°	90
Volume/Å^3	938.92
Z	2
ρ_{calc} / g/cm^3	1.40
μ/mm^{-1}	0.92
F(000)	412.00
Crystal size/mm^3	0.1 x 0.1 x 0.05
Radiation	Mo Kα (λ = 0.71073)
2Θ range for data collection/°	2.997 to 32.360
Index ranges	$-8 \leq h \leq 7$, $-8 \leq k \leq 9$, $-40 \leq l \leq 35$
Reflections collected	25640
Independent reflections	3107
Data/restraints/parameters	3100 / 0 / 136
Goodness-of-fit on F^2	0.997
Final R indexes [I>=2σ (I)]	R_1 = 0.0466, wR_2 = 0.1137
Final R indexes [all data]	R_1 = 0.0674, wR_2 = 0.1233
Largest diff peak/hole/e Å^{-3}	-0.38 / 0.52

Table S2. Bond Lengths (Å) for 22021.

Atom	**Atom**	**Length**
O1	C2	1.226(2)
C2	N3	1.352(1)
C2	C10	1.504(2)
N3	C4	1.411(1)
C4	C5	1.390(2)
C4	C9	1.390(2)
C5	C6	1.392(2)
C6	C7	1.379(2)
C7	C8	1.388(2)
C8	C9	1.386(2)
C10	N11	1.337(2)
C10	C15	1.389(2)

N11	C12	1.344(1)
C12	C13	1.400(2)
C12	C12	1.482(2)
C13	C14	1.381(2)
C14	C15	1.385(2)
O1	C2	1.226(2)
C2	N3	1.352(1)
C2	C10	1.504(2)
N3	C4	1.411(1)
C4	C5	1.390(2)
C4	C9	1.390(2)
C5	C6	1.392(2)
C6	C7	1.379(2)
C7	C8	1.388(2)
C8	C9	1.386(2)
C10	N11	1.337(2)
C10	C15	1.389(2)
N11	C12	1.344(1)
C12	C13	1.400(2)
C13	C14	1.381(2)
C14	C15	1.385(2)

Table S3. Bond Angles (°) for 22021.

Atom	Atom	Atom	Angle
O1	C2	N3	125.6(1)
O1	C2	C10	120.6(1)
N3	C2	C10	113.88(9)
C2	N3	C4	127.41(9)
N3	C4	C5	122.9(1)
N3	C4	C9	117.3(1)
C5	C4	C9	119.8(1)
C4	C5	C6	119.0(1)
C5	C6	C7	121.4(1)
C6	C7	C8	119.3(1)
C7	C8	C9	120.1(1)
C4	C9	C8	120.4(1)
C2	C10	N11	117.4(1)
C2	C10	C15	118.9(1)
N11	C10	C15	123.7(1)
C10	N11	C12	117.84(9)
N11	C12	C13	122.1(1)
N11	C12	C12	116.7(1)

C13	C12	C12	121.2(1)
C12	C13	C14	118.9(1)
C13	C14	C15	119.3(1)
C10	C15	C14	118.1(1)
O1	C2	N3	125.6(1)
O1	C2	C10	120.6(1)
N3	C2	C10	113.88(9)
C2	N3	C4	127.41(9)
N3	C4	C5	122.9(1)
N3	C4	C9	117.3(1)
C5	C4	C9	119.8(1)
C4	C5	C6	119.0(1)
C5	C6	C7	121.4(1)
C6	C7	C8	119.3(1)
C7	C8	C9	120.1(1)
C4	C9	C8	120.4(1)
C2	C10	N11	117.4(1)
C2	C10	C15	118.9(1)
N11	C10	C15	123.7(1)
C10	N11	C12	117.84(9)
C12	C12	N11	116.7(1)
C12	C12	C13	121.2(1)
N11	C12	C13	122.1(1)
C12	C13	C14	118.9(1)
C13	C14	C15	119.3(1)
C10	C15	C14	118.1(1)

[1][PF_6] – 21039

Crystallographic Details. The crystal sample was grown from a mixture of [**1**][BAr^F_4], $OPPh_3$, and H_2^{Ph}bpy-da dissolved in a saturated acetonitrile solution of ammonium hexafluorophosphate. From this sample, a red crystal of approximate dimensions 0.1 mm x 0.1 mm x 0.1 mm was placed onto the tip of a MiTeGen loop before mounting the crystal in a Bruker SMART Apex II diffractometer. Subsequent X-ray study was performed under an N_2 cryo-stream at 150 K.

Crystallographic Details. Preliminary cell constants were first determined using reflections harvested from 3 sets of 12 frames. These sets of frames were positioned so that orthogonal wedges of reciprocal space were surveyed to allow determination of initial orientation matrices from 128 reflections. Next, data collection was performed using a Cu Kα radiation source (graphite monochromator), a theta-dependent frame window of 10-60 seconds, and a detector distance of 4 cm. A randomly oriented region of reciprocal space was surveyed to achieve complete data with a redundancy of 7.8. Sections of frames were collected in 1.0 º steps as ω and φ scans. During reduction, data to a resolution of 0.82 Å were considered. Cell constants after data reduction were calculated from the xyz centroids of 8905 strong reflections after integration (SAINT).[1] Absorption correction was applied to the intensity data (SADABS).[2] For additional crystal and refinement information, refer to Table S4.

Structure Solution and Refinement. A space group of *P2₁/c* was determined based on intensity statistics and systematic absences. Superflip[3] was used to solve the structure which was then refined (full-matrix least-squares) using the Oxford University Crystals software package for Windows.[4] Non-hydrogen atoms were refined with anisotropic displacement parameters before placing hydrogen atoms in ideal geometric positions. Additional refinement cycles then performed in which these hydrogen atoms were refined as riding atoms with individual relative isotropic

displacement parameters. The final full-matrix least-squares refinement converged with R1 = 0.0299 and wR2 = 0.0386 (F^2, all data).

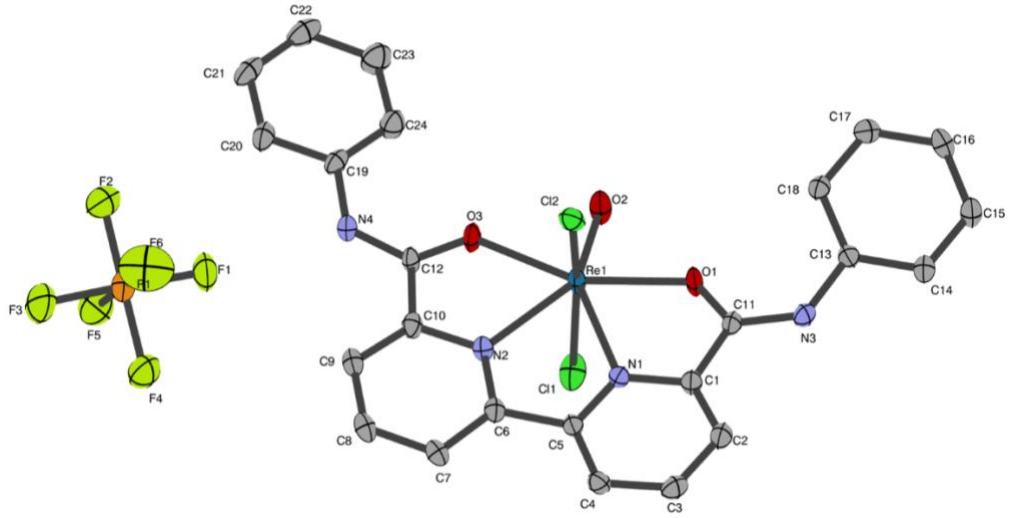

Figure S21. Crystal structure of [**1**][PF_6] with atom labels on the asymmetric unit.

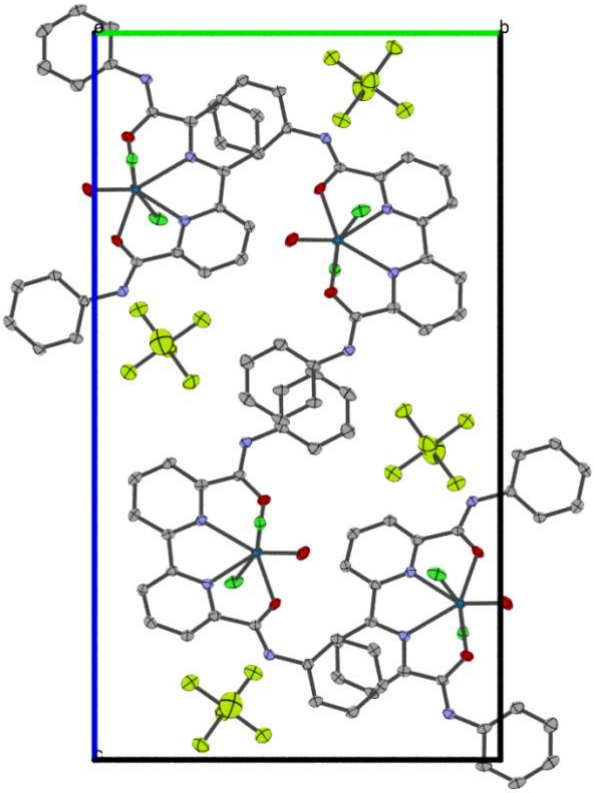

Figure S22. Cell plot of [**1**][PF_6], viewed along a axis.

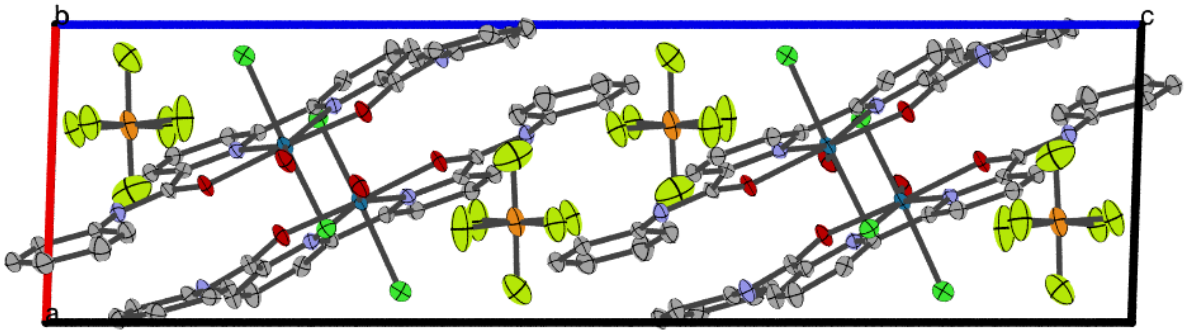

Figure S23. Cell plot of [**1**][PF_6], viewed along b axis.

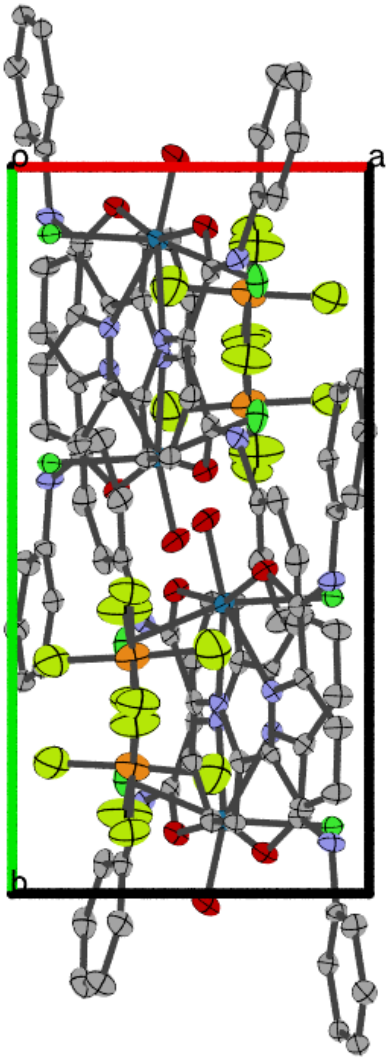

Figure S24. Cell plot of [**1**][PF_6], viewed along c axis.

Table S4. Crystal data and structure refinement for 21039.

Identification code	21039
Empirical formula	$ReCl_2PF_6O_3N_4C_{24}H_{18}$
Formula weight	812.50
Temperature/K	150
Crystal system	Monoclinic
Space group	$P2_1/c$
a/Å	7.0838(2)
b/Å	14.3946(3)
c/Å	25.8235(6)
α/°	90
β/°	91.8555(12)
γ/°	90
Volume/Å^3	2633.18(27)
Z	4
ρ_{calc} / g/cm^3	2.050
μ/mm^{-1}	12.208
F(000)	1568
Crystal size/mm^3	0.1 x 0.1 x 0.1
Radiation	Cu Kα (λ = 1.54178)
2Θ range for data collection/°	3.425 to 72.395
Index ranges	$-8 \leq h \leq 8$, $-17 \leq k \leq 17$, $-30 \leq l \leq 31$
Reflections collected	22708
Independent reflections	5193
Data/restraints/parameters	5145 /8 / 378
Goodness-of-fit on F^2	0.998
Final R indexes [I>=2σ (I)]	$R_1 = 0.0259$, $wR_2 = 0.0386$
Final R indexes [all data]	$R_1 = 0.0299$, $wR_2 = 0.0386$
Largest diff. peak/hole / e Å^{-3}	-0.74 / 1.10

Table S5. Bond Lengths (Å) for 21039.

Atom	Atom	Length
C1	C2	1.380(4)
C1	C11	1.476(4)
C1	N1	1.341(3)
C2	C3	1.384(4)
C3	C4	1.392(4)
C4	C5	1.395(4)
C5	C6	1.466(3)
C5	N1	1.334(4)
C6	C7	1.396(4)
C6	N2	1.344(3)

C7	C8	1.393(4)
C8	C9	1.384(4)
C9	C10	1.383(4)
C10	C12	1.470(4)
C10	N2	1.356(3)
C11	O1	1.255(3)
C11	N3	1.329(3)
C12	O3	1.248(3)
C12	N4	1.335(3)
C13	C14	1.393(4)
C13	C18	1.394(4)
C13	N3	1.426(4)
C14	C15	1.385(4)
C15	C16	1.386(4)
C16	C17	1.388(4)
C17	C18	1.398(4)
C19	C20	1.395(4)
C19	C24	1.380(4)
C19	N4	1.430(4)
C20	C21	1.385(4)
C21	C22	1.377(4)
C22	C23	1.388(4)
C23	C24	1.396(4)
O1	Re1	2.129(2)
O2	Re1	1.683(2)
O3	Re1	2.132(2)
N1	Re1	2.302(2)
N2	Re1	2.287(2)
Cl1	Re1	2.3479(7)
Cl2	Re1	2.3564(6)
F1	P1	1.598(2)
F2	P1	1.594(3)
F3	P1	1.602(2)
F4	P1	1.604(2)
F5	P1	1.611(2)
F6	P1	1.581(3)

Table S6. Bond Angles (°) for 21039.

Atom	Atom	Atom	Angle
C2	C1	C11	126.7(2)
C2	C1	N1	123.1(2)
C11	C1	N1	110.2(2)
C1	C2	C3	118.3(3)

C2	C3	C4	119.0(3)
C3	C4	C5	119.0(2)
C4	C5	C6	124.0(2)
C4	C5	N1	121.6(2)
C6	C5	N1	114.3(2)
C5	C6	C7	124.2(2)
C5	C6	N2	113.3(2)
C7	C6	N2	122.5(2)
C6	C7	C8	118.4(2)
C7	C8	C9	119.3(2)
C8	C9	C10	118.9(2)
C9	C10	C12	127.5(2)
C9	C10	N2	122.6(2)
C12	C10	N2	109.8(2)
C1	C11	O1	116.4(2)
C1	C11	N3	121.1(2)
O1	C11	N3	122.6(2)
C10	C12	O3	116.6(2)
C10	C12	N4	120.5(2)
O3	C12	N4	122.9(2)
C14	C13	C18	120.7(2)
C14	C13	N3	116.6(2)
C18	C13	N3	122.6(2)
C13	C14	C15	119.6(3)
C14	C15	C16	120.3(3)
C15	C16	C17	120.2(3)
C16	C17	C18	120.1(2)
C13	C18	C17	119.1(2)
C20	C19	C24	121.1(3)
C20	C19	N4	115.1(2)
C24	C19	N4	123.8(2)
C19	C20	C21	119.0(3)
C20	C21	C22	120.7(3)
C21	C22	C23	120.0(3)
C22	C23	C24	120.2(3)
C19	C24	C23	119.0(3)
C11	O1	Re1	125.3(2)
C12	O3	Re1	125.5(2)
C1	N1	C5	118.9(2)
C1	N1	Re1	119.0(2)
C5	N1	Re1	122.1(2)
C6	N2	C10	118.2(2)
C6	N2	Re1	122.7(2)
C10	N2	Re1	119.1(2)

C11	N3	C13	126.6(2)
C12	N4	C19	127.7(2)
O1	Re1	O2	77.45(9)
O1	Re1	O3	155.35(8)
O1	Re1	N1	68.57(8)
O1	Re1	N2	135.97(8)
O1	Re1	Cl1	93.36(6)
O1	Re1	Cl2	90.11(6)
O2	Re1	O3	77.97(9)
O2	Re1	N1	146.01(9)
O2	Re1	N2	146.56(9)
O2	Re1	Cl1	98.97(7)
O2	Re1	Cl2	98.53(7)
O3	Re1	N1	136.01(8)
O3	Re1	N2	68.59(8)
O3	Re1	Cl1	92.18(6)
O3	Re1	Cl2	91.78(6)
N1	Re1	N2	67.42(8)
N1	Re1	Cl1	82.85(6)
N1	Re1	Cl2	82.47(6)
N2	Re1	Cl1	82.64(6)
N2	Re1	Cl2	82.96(6)
Cl1	Re1	Cl2	162.50(2)
F1	P1	F2	90.0(1)
F1	P1	F3	177.4(1)
F1	P1	F4	89.4(1)
F1	P1	F5	90.8(1)
F1	P1	F6	92.0(1)
F2	P1	F3	91.1(1)
F2	P1	F4	178.9(1)
F2	P1	F5	89.8(1)
F2	P1	F6	91.3(2)
F3	P1	F4	89.5(1)
F3	P1	F5	86.8(1)
F3	P1	F6	90.3(2)
F4	P1	F5	89.4(1)
F4	P1	F6	89.6(1)
F5	P1	F6	177.0(2)

[Na•a18c6][2] – 21064

Crystallographic Details. The crystal sample was grown via addition of excess aza-18-crown-6 to a suspension of [Na][**2**]. The resulting mixture was filtered, and X-ray quality crystals were obtained via vapor diffusion of Et_2O into the filtrate at -30 °C. From this sample, an orange crystal of approximate dimensions 0.1 mm x 0.1 mm x 0.1 mm was placed onto the tip of a MiTeGen loop before mounting the crystal in a Bruker SMART Apex II diffractometer. Subsequent X-ray study was performed at room temperature.

Structure Solution and Refinement. A dark orange crystal of approximate dimensions 0.1 mm x 0.1 mm x 0.1 mm was placed onto the tip of a MiTeGen loop before mounting the crystal in a Bruker SMART Apex II diffractometer. Subsequent X-ray study was performed at room temperature. Preliminary cell constants were first determined using reflections harvested from 3 sets of 12 frames. These sets of frames were positioned so that orthogonal wedges of reciprocal space were surveyed to allow determination of initial orientation matrices from 137 reflections. Next, data collection was performed assuming a $P2_1/c$ space group using a Cu Kα radiation source (graphite monochromator), a theta-dependent frame window between 10-30 seconds, and a detector distance of 4 cm. Sections of frames were collected in 0.5º steps as ω and φ scans. During reduction, data to a resolution of 0.84 Å were considered. Cell constants after data reduction were calculated from the xyz centroids of 7221 strong reflections after integration (SAINT).[1] Absorption correction was applied to the intensity data (SADABS).[2] For additional crystal and refinement information, refer to Table S7.

Structure Solution and Refinement. A space group of $P2_1/c$ was determined based on intensity statistics and systematic absences. SHELXT[5] was used to solve the structure which was then

refined (full-matrix least-squares) using the Oxford University Crystals software package for Windows.[4] Non-hydrogen atoms were refined with anisotropic displacement parameters before placing hydrogen atoms in ideal geometric positions. Additional refinement cycles then performed in which these hydrogen atoms were refined as riding atoms with individual relative isotropic displacement parameters. The final full-matrix least-squares refinement converged with R1 = 0.1059 and wR2 = 0.2546 (F^2, all data).

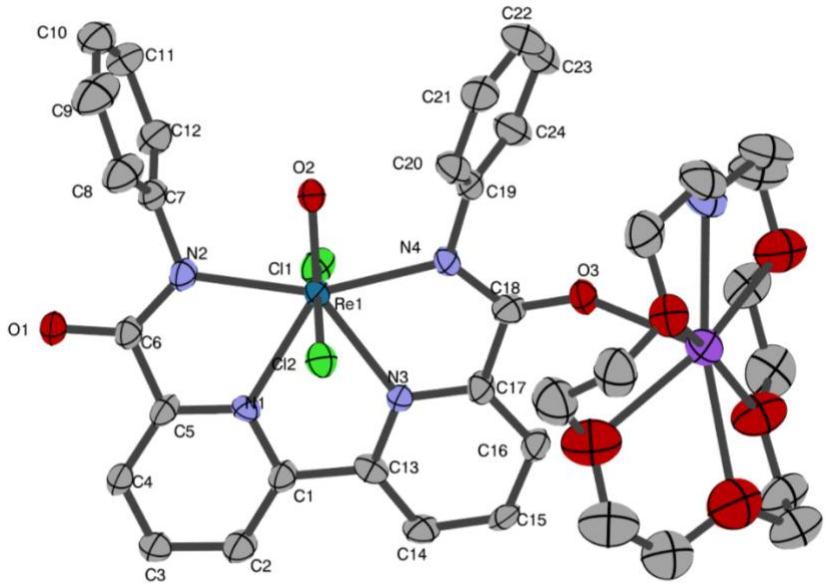

Figure S25. Crystal structure of [Na•a18c6][**2**] with atom labels on the [Re(^{Ph}bpy-da)(O)$(Cl)_2$]$^-$ fragment of the asymmetric unit.

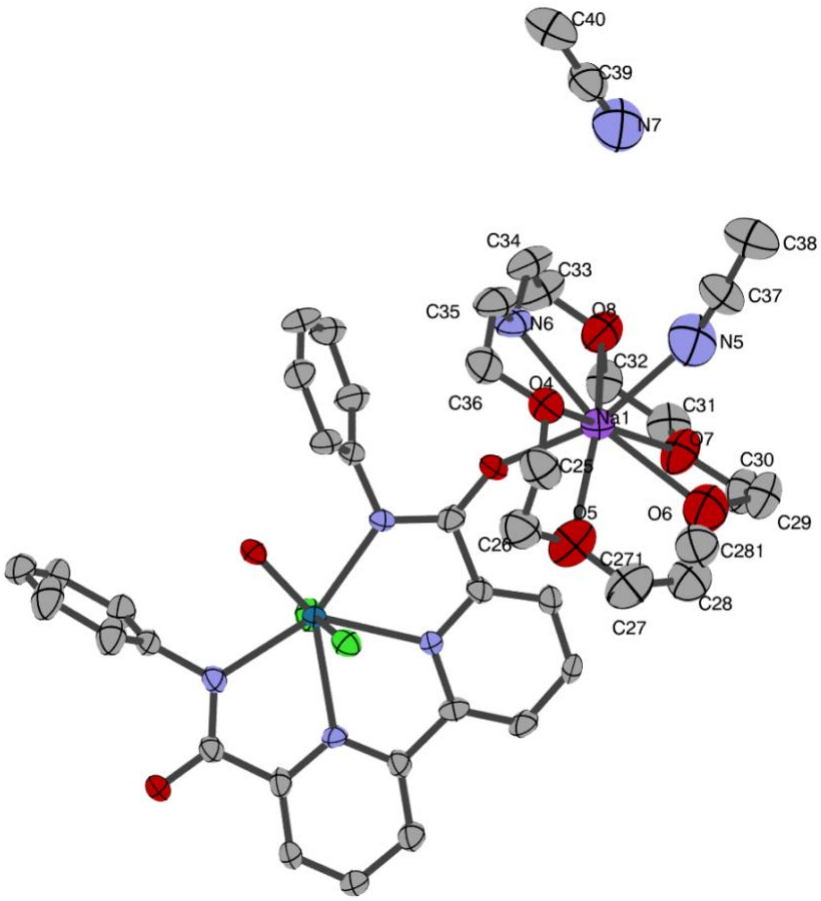

Figure S26. Crystal structure of [Na•a18c6][**2**] with atom labels on the $[Na•a18c6]^{+}$ fragment and additional acetonitrile molecules of the asymmetric unit.

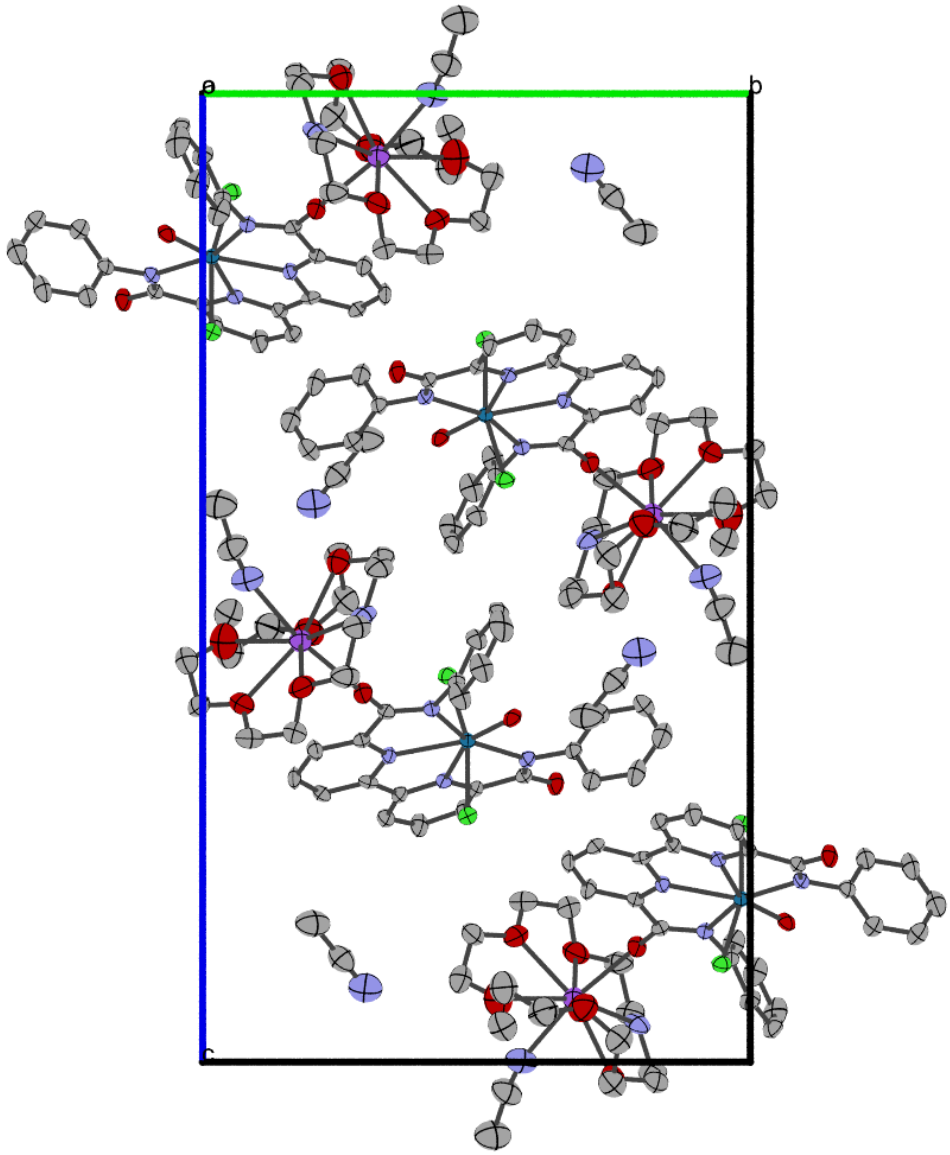

Figure S27. Cell plot of [Na•a18c6][**2**], viewed along a axis.

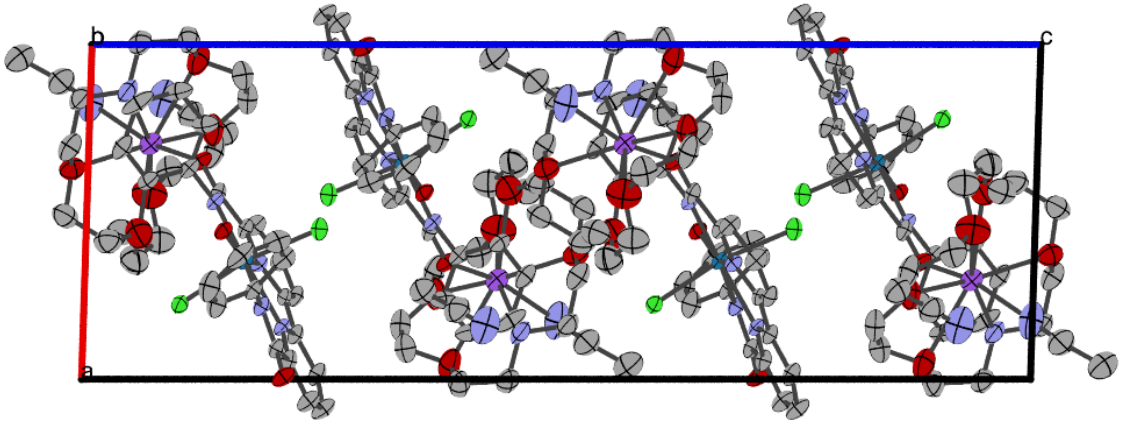

Figure S28. Cell plot of [Na•a18c6][**2**], viewed along b axis.

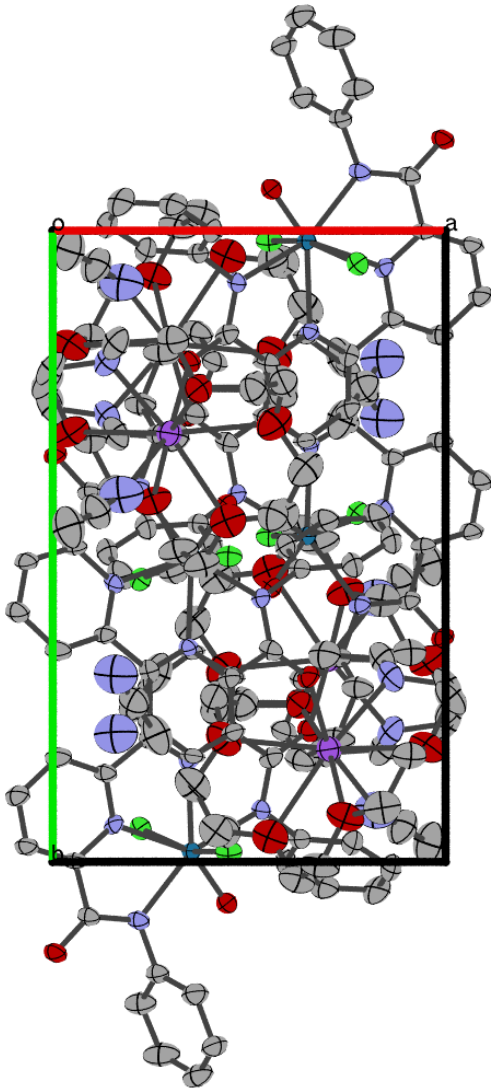

Figure S29. Cell plot of [Na•a18c6][**2**], viewed along c axis.

Table S7. Crystal data and structure refinement for 21064.

Identification code	21064
Empirical formula	$ReCl_2NaO_8N_7C_{40}H_{46}$
Formula weight	1033.95
Temperature/K	298
Crystal system	Monoclinic
Space group	$P2_1/c$
a/Å	9.821(2)
b/Å	15.764(4)
c/Å	27.909(6)
α/°	90
β/°	91.793(14)
γ/°	90
Volume/Å^3	4318.6(17)
Z	4
ρ_{calc} / g/cm^3	1.590
μ/mm^{-1}	7.233
F(000)	2080
Crystal size/mm^3	0.1 x 0.1 x 0.1
Radiation	Cu Kα (λ = 1.54178)
2Θ range for data collection/°	3.168 to 71.670
Index ranges	$-11 \leq h \leq 11$, $-18 \leq k \leq 18$, $-27 \leq l \leq 32$
Reflections collected	17769
Independent reflections	7716
Data/restraints/parameters	7682 / 254 / 555
Goodness-of-fit on F^2	0.994
Final R indexes [I>=2σ (I)]	R_1 = 0.0886, wR_2 = 0.1853
Final R indexes [all data]	R_1 = 0.0733, wR_2 = 0.1752
Largest diff. peak/hole / e Å^{-3}	-3.39 / 4.79

Table S8. Bond Lengths (Å) for 21064.

Atom	**Atom**	**Length**
Re1	Cl1	2.386(2)
Re1	Cl2	2.368(2)
Re1	O2	1.687(6)
Re1	N1	2.319(7)
Re1	N2	2.229(7)
Re1	N3	2.305(8)
Re1	N4	2.212(7)
Na1	O3	2.388(8)
Na1	O4	2.661(9)
Na1	O5	2.66(1)
Na1	O6	2.64(1)

Na1	O7	2.512(9)
Na1	O8	2.83(1)
Na1	N5	2.61(2)
Na1	N6	2.48(1)
O1	C6	1.25(1)
O3	C18	1.25(1)
O4	C25	1.401(9)
O4	C36	1.40(1)
O5	C26	1.40(1)
O5	C27	1.39(1)
O6	C28	1.40(2)
O6	C29	1.40(1)
O7	C30	1.39(1)
O7	C31	1.40(1)
O8	C32	1.392(9)
O8	C33	1.39(1)
N1	C1	1.36(1)
N1	C5	1.35(1)
N2	C6	1.32(1)
N2	C7	1.43(1)
N3	C13	1.36(1)
N3	C17	1.35(1)
N4	C18	1.33(1)
N4	C19	1.426(9)
N5	C37	1.16(2)
N6	C34	1.47(2)
N6	C35	1.48(1)
C1	C2	1.39(1)
C1	C13	1.46(1)
C2	C3	1.41(1)
C3	C4	1.36(1)
C4	C5	1.38(1)
C5	C6	1.48(1)
C7	C8	1.39(1)
C7	C12	1.39(1)
C8	C9	1.40(1)
C9	C10	1.38(1)
C10	C11	1.37(1)
C11	C12	1.40(1)
C13	C14	1.38(1)
C14	C15	1.38(1)
C15	C16	1.40(1)
C16	C17	1.39(1)
C17	C18	1.49(1)

C19	C20	1.39(1)
C19	C24	1.391(9)
C20	C21	1.40(1)
C21	C22	1.38(1)
C22	C23	1.38(1)
C23	C24	1.40(1)
C25	C26	1.48(1)
C27	C28	1.47(2)
C29	C30	1.47(1)
C31	C32	1.47(1)
C33	C34	1.47(1)
C35	C36	1.48(1)
C37	C38	1.46(2)
N7	C39	1.16(2)
C39	C40	1.42(2)

Table S9. Bond Angles (°) for 21064.

Atom	Atom	Atom	Angle
Cl1	Re1	Cl2	162.60(8)
Cl1	Re1	O2	97.9(2)
Cl1	Re1	N1	84.0(2)
Cl1	Re1	N2	91.7(2)
Cl1	Re1	N3	81.1(2)
Cl1	Re1	N4	93.1(2)
Cl2	Re1	O2	99.5(2)
Cl2	Re1	N1	82.0(2)
Cl2	Re1	N2	92.6(2)
Cl2	Re1	N3	83.9(2)
Cl2	Re1	N4	89.6(2)
O2	Re1	N1	146.5(3)
O2	Re1	N2	78.6(3)
O2	Re1	N3	146.9(3)
O2	Re1	N4	78.4(3)
N1	Re1	N2	67.9(2)
N1	Re1	N3	66.6(2)
N1	Re1	N4	135.0(2)
N2	Re1	N3	134.4(2)
N2	Re1	N4	156.9(2)
N3	Re1	N4	68.6(2)
O3	Na1	O4	99.7(3)
O3	Na1	O5	78.3(3)
O3	Na1	O6	121.1(3)
O3	Na1	O7	95.2(3)
O3	Na1	O8	82.4(3)

O3	Na1	N5	162.7(4)
O3	Na1	N6	75.7(3)
O4	Na1	O5	65.0(3)
O4	Na1	O6	100.3(3)
O4	Na1	O7	161.9(3)
O4	Na1	O8	131.4(3)
O4	Na1	N5	77.5(4)
O4	Na1	N6	68.4(3)
O5	Na1	O6	61.9(3)
O5	Na1	O7	108.7(3)
O5	Na1	O8	157.0(3)
O5	Na1	N5	114.8(4)
O5	Na1	N6	120.8(3)
O6	Na1	O7	62.9(3)
O6	Na1	O8	120.2(3)
O6	Na1	N5	76.0(4)
O6	Na1	N6	161.9(4)
O7	Na1	O8	60.7(3)
O7	Na1	N5	91.1(4)
O7	Na1	N6	125.9(3)
O8	Na1	N5	86.8(4)
O8	Na1	N6	65.2(3)
N5	Na1	N6	87.6(4)
Na1	O3	C18	144.3(6)
Na1	O4	C25	113.4(5)
Na1	O4	C36	106.8(5)
C25	O4	C36	116.3(7)
Na1	O5	C26	108.7(7)
Na1	O5	C27	119.0(8)
C26	O5	C27	117(1)
Na1	O6	C28	116.6(8)
Na1	O6	C29	112.1(7)
C28	O6	C29	118(1)
Na1	O7	C30	122.5(6)
Na1	O7	C31	122.2(6)
C30	O7	C31	115.3(8)
Na1	O8	C32	100.2(5)
Na1	O8	C33	106.1(6)
C32	O8	C33	116.9(8)
Re1	N1	C1	122.8(5)
Re1	N1	C5	118.8(6)
C1	N1	C5	118.3(7)
Re1	N2	C6	124.9(6)
Re1	N2	C7	118.8(5)

C6	N2	C7	116.2(7)
Re1	N3	C13	123.5(5)
Re1	N3	C17	119.2(5)
C13	N3	C17	117.1(7)
Re1	N4	C18	125.4(6)
Re1	N4	C19	120.1(5)
C18	N4	C19	114.5(7)
Na1	N5	C37	165(1)
Na1	N6	C34	115.6(7)
Na1	N6	C35	112.8(6)
C34	N6	C35	114.4(9)
N1	C1	C2	122.5(8)
N1	C1	C13	113.4(7)
C2	C1	C13	124.2(8)
C1	C2	C3	118.0(9)
C2	C3	C4	119(1)
C3	C4	C5	121.3(9)
N1	C5	C4	121.4(8)
N1	C5	C6	114.8(8)
C4	C5	C6	123.8(9)
O1	C6	N2	128.7(8)
O1	C6	C5	118.9(8)
N2	C6	C5	112.2(8)
N2	C7	C8	121.3(7)
N2	C7	C12	118.3(7)
C8	C7	C12	120.4(7)
C7	C8	C9	119.4(8)
C8	C9	C10	120.1(8)
C9	C10	C11	120.6(8)
C10	C11	C12	120.1(8)
C7	C12	C11	119.4(8)
N3	C13	C1	113.2(7)
N3	C13	C14	123.0(8)
C1	C13	C14	123.7(8)
C13	C14	C15	119.2(8)
C14	C15	C16	119.0(8)
C15	C16	C17	118.2(8)
N3	C17	C16	123.5(8)
N3	C17	C18	114.7(8)
C16	C17	C18	121.8(8)
O3	C18	N4	129.1(8)
O3	C18	C17	118.9(8)
N4	C18	C17	112.0(8)
N4	C19	C20	119.8(6)

N4	C19	C24	119.7(6)
C20	C19	C24	120.4(7)
C19	C20	C21	119.4(7)
C20	C21	C22	120.1(8)
C21	C22	C23	120.7(9)
C22	C23	C24	120.2(8)
C19	C24	C23	119.3(8)
O4	C25	C26	111.8(7)
O5	C26	C25	111.7(9)
O5	C27	C28	112(1)
O6	C28	C27	112(1)
O6	C29	C30	111.7(9)
O7	C30	C29	111.7(9)
O7	C31	C32	111.8(8)
O8	C32	C31	111.7(7)
O8	C33	C34	111.8(9)
N6	C34	C33	109.0(9)
N6	C35	C36	110.8(8)
O4	C36	C35	111.8(8)
N5	C37	C38	171(2)
N7	C39	C40	179(2)

IV. Cambridge Crystallographic Database Centre Comparisons

Table S10. Re≡O Bond Distances in Pentagonal Bipyramidal Re^{V} Terminal Oxo Complexes.

Reference Code	Re≡O Distance (Å)
KUKROX[6]	1.666
LAFLIO[7]	1.752
SOSQOG[8]	1.662
SOSQUM[8]	1.688
SOTFIQ[8]	1.690
SOZGIX[9]	1.693
Average (σ)	**1.692 (0.029)**

Table S11. Re–N(bpy) and Re≡O Bond Distances in Octahedral Re^{V} Terminal Oxo Complexes.

Reference Code	Re–N(bpy) Distance; *trans* to oxo (Å)	Re–N(bpy) Distance; *cis* to oxo (Å)	Re≡O Distance (Å)
BAWSAU[10]	2.257	2.139	1.689
ILIBAG[11]	2.233	2.197	1.701
ILIBEK[11]	2.256	2.191	1.691
KATHOC[12]	2.359	2.128	1.682
QUBJEC[13]	2.284	2.199	1.669
QUBJOM[13]	2.286	2.204	1.687
QUBJUS[13]	2.296	2.151	1.689
VEQLAE[14]	2.322	2.134	1.671
VEQLEI[14]	2.264	2.050	1.644
VEQLIM[14]	2.303	2.132	1.674
XOLKIS[15]	2.275	2.184	1.687
YILWAS[16]	2.266	2.201	1.701
Average (σ)	**2.282 (0.034)**	**2.159 (0.044)**	**1.682 (0.015)**

V. Computational Information

DFT calculations were done using Gaussian 16.[17] The geometries were optimized to minima or transition states in the gas phase using the M06L functional and the 6-311G(d,p) basis set on the main group elements.[18,19] Rhenium carried the SDD relativistic ECP and associated basis set augmented with an f polarization function from the Frenking basis set (exponent = 0.86).[20,21] This level was also used to calculate the harmonic vibrational frequencies and to obtain the correction terms to the standard state Gibbs free energies at 1 M and 298 K (G^{o}).[22] Final energies were obtained by single point calculations on the gas phase geometries using the def2-TZVP basis set on the non-metals and the def2-QZVP basis set and associated ECP on rhenium,[23] in a polarizable continuum representing THF as solvent.[24]

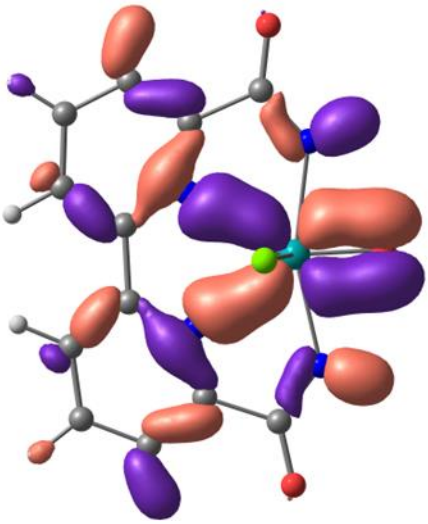

Figure S30. Canonical orbital rendering of MO corresponding to Re d_{xz} parent bonding orbital. MO simplified by replacement of N–Ph with N–H. MO rendered with isosurface value of 0.3 e Å^{-3}.

VI. References

1 Bruker Analytical X-Ray Systems, .

2 R. H. Blessing, *Acta Crystallogr. Sect. A Found. Crystallogr.*, 1995, **51**, 33–38.

3 L. Palatinus and G. Chapuis, *J. Appl. Crystallogr.*, 2007, **40**, 786–790.

4 P. W. Betteridge, J. R. Carruthers, R. I. Cooper, K. Prout and D. J. Watkin, *J. Appl. Crystallogr.*, 2003, **36**, 1487–1487.

5 G. M. Sheldrick, *Acta Crystallogr. Sect. A Found. Crystallogr.*, 2015, **71**, 3–8.

6 C. M. Che, Y. P. Wang, K. S. Yeung, K. Y. Wong and S. M. Peng, *J. Chem. Soc. Dalt. Trans.*, 1992, **524**, 2675–2677.

7 H.-Y. Jin, S. Ikari, K. Kobayashi, K. Umakoshi, H. Sugimoto, A. Mitani, M. Abe, Y. Sasaki and T. Ito, *Bull. Chem. Soc. Jpn.*, 2004, **77**, 1139–1146.

8 L. Xu, I. A. Setyawati, J. Pierreroy, M. Pink, V. G. Young, B. O. Patrick, S. J. Rettig and C. Orvig, *Inorg. Chem.*, 2000, **39**, 5958–5963.

9 M. Leeaphon, P. E. Fanwick and R. A. Walton, *Inorg. Chem.*, 1991, **30**, 4986–4995.

10 B. Machura, J. O. Dzięgielewski, R. Kruszynski, T. J. Bartczak and J. Kusz, *Polyhedron*, 2003, **22**, 2573–2580.

11 M. Papachristou, I. C. Pirmettis, C. Tsoukalas, D. Papagiannopoulou, C. Raptopoulou, A. Terzis, C. I. Stassinopoulou, E. Chiotellis, M. Pelecanou and M. Papadopoulos, *Inorg. Chem.*, 2003, **42**, 5778–5784.

12 W. A. Herrmann, J. G. Kuchler, G. Weischselbaumer, E. Herdtweck and P. Kiprof, *J. Organomet. Chem.*, 1989, **372**, 351–370.

13 J.-H. Jung, D. M. Hoffman and T. R. Lee, *J. Organomet. Chem.*, 2000, **599**, 112–122.

14 J. H. Jung, T. A. Albright, D. M. Hoffman and T. R. Lee, *J. Chem. Soc. - Dalt. Trans.*, 1999, **2**, 4487–4494.

15 J. H. Espenson, X. Shan, D. W. Lahti, T. M. Rockey, B. Saha and A. Ellern, *Inorg. Chem.*, 2001, **40**, 6717–6724.

16 D. Papagiannopoulou, I. Pirmettis, M. Pelecanou, D. Komiotis, M. Sagnou, D. Benaki, C. P. Raptopoulou, A. Terzis and M. S. Papadopoulos, *Inorganica Chim. Acta*, 2007, **360**, 3597–3602.

17 M. J. Frisch, 2016.

18 Y. Zhao and D. G. Truhlar, *J. Chem. Phys.*, 2006, **125**, 194101.

19 R. Krishnan, J. S. Binkley, R. Seeger and J. A. Pople, *J. Chem. Phys.*, 1980, **72**, 650–654.

20 D. Andrae, U. Häußermann, M. Dolg, H. Stoll and H. Preuß, *Theor. Chim. Acta*, 1990, **77**, 123–141.

21 A. W. Ehlers, M. Böhme, S. Dapprich, A. Gobbi, A. Höllwarth, V. Jonas, K. F. Köhler, R. Stegmann, A. Veldkamp and G. Frenking, *Chem. Phys. Lett.*, 1993, **208**, 111–114.

22 J. H. Jensen, *Phys. Chem. Chem. Phys.*, 2015, **17**, 12441–12451.

23 B. P. Pritchard, D. Altarawy, B. Didier, T. D. Gibson and T. L. Windus, *J. Chem. Inf. Model.*, 2019, **59**, 4814–4820.

24 A. V. Marenich, C. J. Cramer and D. G. Truhlar, *J. Phys. Chem. B*, 2009, **113**, 6378–6396.